PROCEDURE OF SHAKING AND TSUNAMI VULNERABILITY ASSESSMENTS OF TSUNAMI EVACUATION SHELTERS

A procedure to carry out vulnerability assessments of TESs due to shaking and tsunami is presented in Figure 1. First, earthquake and tsunami simulations are conducted. A ground motion prediction equations (GMPE) developed by Abrahamson et al. (2016) is adopted to carry out the earthquake simulation. Noting that, the source scenarios for the seismic and tsunami simulations are the same. Second, the vulnerability assessment is carried out. The building vulnerability is assessed by determining the probability of a building experiencing specific damage states for a given hazard level, e.g. spectral acceleration (Sa) at a certain vibration period and spectral displacement for shaking and maximum tsunami depth (h) for tsunami (Rossetto and Elnashai, 2003; Sabandi et al., 2004; Porter et al., 2007; Ahmad et al., 2015; De Risi and Goda, 2016). Subsequently, the fragility models for both earthquake and tsunami vulnerability assessment are adopted. Since the tsunami is a secondary hazard triggered by an earthquake fault rupture, the seismic vulnerability assessment of TESs is carried out prior to the tsunami vulnerability assessment (see Figure 1). Detail procedures for the TES earthquake-tsunami hazard and vulnerability assessments are presented below.

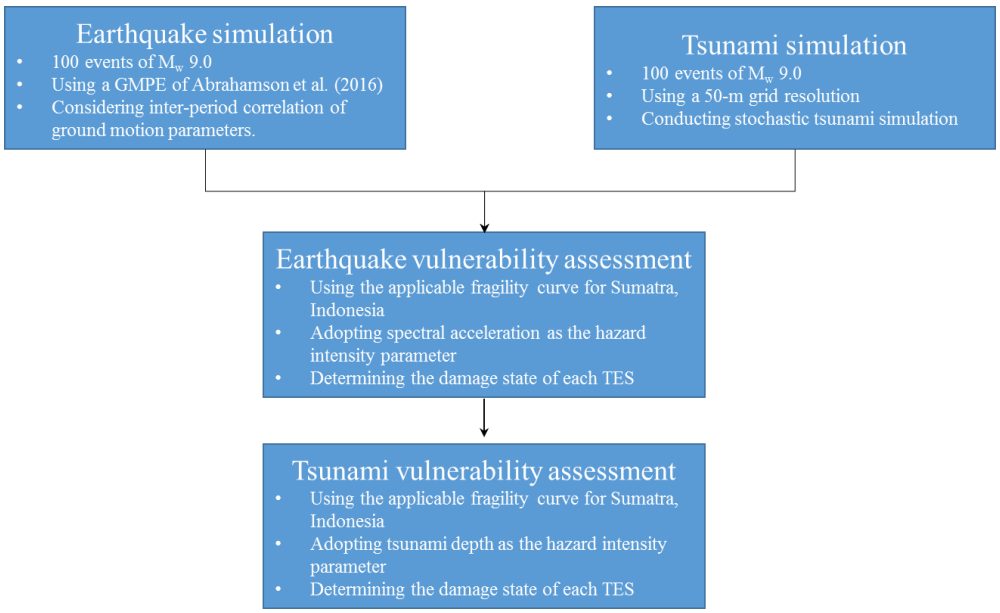

Figure 1. Procedure of earthquake and tsunami hazard and vulnerability assessment of tsunami evacuation shelters.

1. EARTHQUAKE SIMULATION

Seismic intensity measures for a given earthquake scenario at the TEBs can be effectively estimated using ground motion prediction equations (Wald et al., 2016; Douglas, 2017). In this study, spectral acceleration (Sa) is selected as the intensity measure because most of empirical fragility models for buildings (e.g. HAZUS; Rossetto and Elnashai, 2003; Ahmad et al., 2014) use this parameter. Among existing GMPEs (e.g. Chang et al., 2001; Kataoka et al., 2006; Goda and Atkinson, 2009; Morikawa and Fujiwara, 2013; Abrahamson et al., 2016), a relationship by Abrahamson et al. (2016) is adopted for three reasons: (1) it is developed for global subduction environment (rather than specific geographical regions) and therefore, is applicable to mega-thrust interface subduction earthquakes in Sumatra, Indonesia, (2) including two of the most recent significant subduction earthquakes, i.e. the 2010 Maule, Chile and the 2011 Tohoku, Japan earthquakes, and (3) developed from an extensive ground motion dataset for subduction earthquakes around the world.

An equation to model the ground motion intensity of an interface subduction earthquake is the following:

$$\ln(S_a) = \theta_1 + \theta_4 \cdot \Delta C_1 + [\theta_2 + \theta_3 \cdot (M_w - 7.8)] \cdot \ln\{R + C_4 \cdot \exp[\theta_9 \cdot (M_w - 6)]\} + \theta_6 \cdot R + f_{MAG}(M_w) + f_{FABA}(R) + f_{SITE}(PGA_{1000}, V_{s30}) + \sigma \cdot \varepsilon \quad (1)$$

where ln is the natural logarithm, Mw is … R (km) is the closest distance to the rupture area, V_{S30} (m/s) is the average shear wave velocity in the uppermost 30 m of soil column, PGA_{1000} is the mean peak ground acceleration (PGA) value corresponding to V_{S30} = 1000 m/s, σ is the total standard deviation (SD), and ε is the Gaussian error term represented by zero mean and unit SD. The magnitude function is shown below:

$$f_{MAG}(M) = \begin{cases} \theta_4 \cdot [M_w - (7.8 + \Delta C_1)] + \theta_{13} \cdot (10 - M)^2 & for\ M_w \leq 7.8 + \Delta C_1 \\ \theta_5 \cdot [M_w - (7.8 + \Delta C_1)] + \theta_{13} \cdot (10 - M)^2 & for\ M_w \leq 7.8 + \Delta C_1 \end{cases} \quad (2)$$

where ΔC_1 represents the epistemic uncertainty to control the magnitude scaling. $f_{FABA}(R)$ is the forearc/backarc terms which is equal to 0 for forearc or unknown site and one for backarc. Because Padang is in the forearc region of the Sumtara subduction zone, $f_{FABA}(R)$ is set to 0.

Finally, the site response scaling is presented by:

$$f_{SITE} = \theta_{12} \cdot \ln\left(\frac{\min(V_{S30}, 1000)}{V_{lin}}\right) - b \cdot \ln(PGA_{1000} + c) + b \cdot \ln\left[PGA_{1000} + c \cdot \left(\frac{\min(V_{S30}, 1000)}{V_{lin}}\right)^n\right] \qquad for\ V_{S30} < V_{lin}$$

$$f_{SITE} = \theta_{12} \cdot \ln\left(\frac{\min(V_{S30},1000)}{V_{lin}}\right) + b \cdot n \cdot \ln\left(\frac{\min(V_{S30},1000)}{V_{lin}}\right) \qquad for\ V_{S30} \geq V_{lin} \qquad (3)$$

All model coefficients for Eqs 1-3 can be found in Abrahamson et al. (2016).

Three parameters are needed as input to simulate the interface megathrust earthquake including magnitude, rupture distance, and shear wave velocity for the considered site. For the TES assessment purposes, only the worst magnitude earthquake scenario is considered (Mw 9.0). On the other hand, the rupture distance is determined based on the closest distance between the location of interest and the rupture areas. Since the locations of TEBs are relatively close (the maximum distance among the TEB is less than 3 km) and this is significantly smaller than the distance between Padang and the rupture plane, seismic vulnerability assessment is conducted for a single representative site in Padang. Subsequently, the rupture distance to the site for the worst case is 55 km calculated from the smallest distance from the source to site of the 100 earthquake scenarios. On the other hand, the longest distance from the source to site among the 100 scenarios is ~100 km. Moreover, V_{S30} in coastal areas of Padang ranges from 200 m/s to 400 m/s (Han et al., 2012; Putra et al., 2014) and hence, V_{S30} of 300 m/s is used in this study. Finally, to include the uncertainty of the prediction equation for multiple spectral acceleration ordinates, a multivariate lognormal distribution is adopted. The median values of spectral acceleration at different vibration periods (at a site of interest) are evaluated using the GMPE with the three parameters, whereas their covariance are based on interperiod correlation of

ground motion parameters $\rho(T_1, T_2)$ (see Baker and Cornell, 2006). The correlation coefficient matrix has diagonal elements equal to 1 and off-diagonal elements equal to the correlation coefficient, ρ. It was calculated based on the following equation (Goda and Atkinson, 2009):

$$\rho(T_1,T_2) = \frac{1}{3}\left(1 - cos\left\{\frac{\pi}{2} - \left[\theta_1 + \theta_2 I_{T_{min<0.25}} \times \left(\frac{T_{min}}{T_{max}}\right)^{\theta_3} log_{10}\left(\frac{T_{min}}{0.25}\right)\right] log_{10}\left(\frac{T_{max}}{T_{min}}\right)\right\}\right) + \frac{1}{3}\left\{1 + cos\left[-1.5 log_{10}\left(\frac{T_{max}}{T_{min}}\right)\right]\right\} \quad (4)$$

where θ_1, θ_2, and θ_3 are the model parameters ($\theta_1 = 1.374, \theta_2 = 5.586$, and $\theta_3 = 0.728$), T_{max} and T_{min} are the maximum and the minimum value of T_1 and T_2, respectively and $I_{T_{min<0.25}}$ is the indicator function that equals one if $T_{min} < 0.25$ sec and equals zero otherwise. Equation (4) was developed based on subduction earthquake records from Japan; thus, it is considered to be applicable to subduction earthquakes in Sumatra.

2. SEISMIC AND TSUNAMI VULNERABILITY ASSESSMENTS

For seismic vulnerability assessment, the fragility curves developed by Federal Emergency Management Agency (FEMA), i.e. HAZUS, is adopted to assess the vulnerability of TESs in Padang because of the following reasons:

1. New Indonesian Earthquake Resistance Building Code (SNI-1726: 2012) mostly adopted the U.S. seismic design documents, i.e. FEMA P7502009, regarding earthquake provisions for new building and other structures, and ASCE/SEI 7-10 for minimum design load criterion (SNI-1726: 2012; Wijayanti et al., 2015; Sengara et al., 2016; Douglas and Gkimprixis, 2017).
2. HAZUS is a well-established earthquake loss estimation framework and has been implemented in several earthquake prone-countries for seismic risk assessment purposes, e.g., Haiti, Puerto Rico, France, Romania, Austria and Indonesia (Kulmesh, 2010; Peterson and Small, 2012; Wijayanti et al., 2015; Sengara et al., 2016; Douglas and Gkimprixis, 2017).

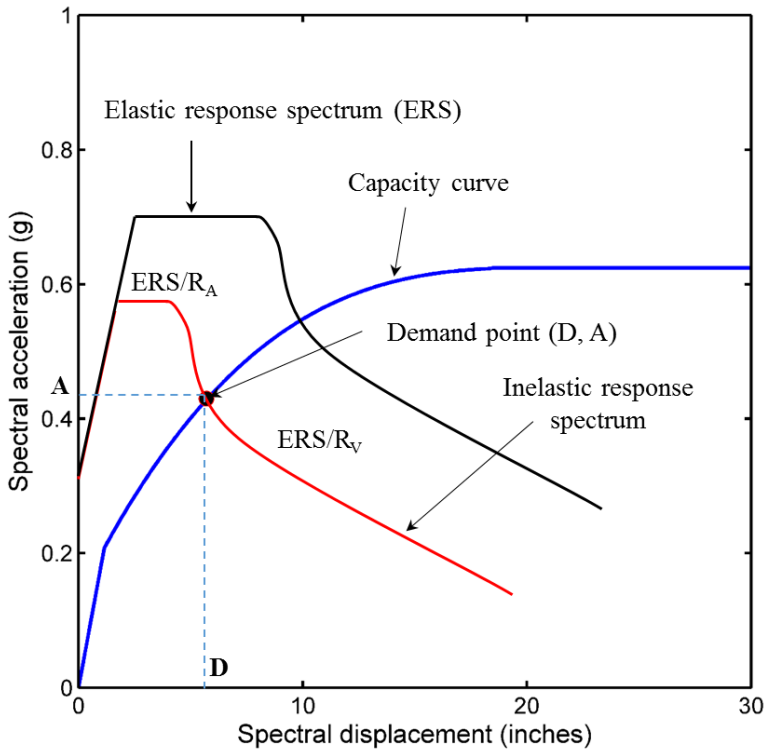

Figure 2. Example of Capacity Spectrum Method used in HAZUS.

Figure 2 illustrates the procedure for developing an inelastic response (demand) spectrum from the elastic response (input) spectrum in HAZUS. First, the acceleration-period response spectrum is generated from the earthquake simulation. It is further converted into the Acceleration-Displacement Response Spectra (ADRS). This ADRS is then defined as the Elastic Response Spectrum (ERS). Second, the demand spectrum is calculated by dividing the ERS by the reduction factors (i.e. R_A at periods of constant acceleration and R_V at periods of constant velocity). Noting that the reduction factors in HAZUS are equal to the reciprocal of SR_A and SR_V in ATC-40 (Applied Technology Council, 1996). For essential and average buildings (type B) the SR_A and SR_V should be less than 2.27 and 1.79, respectively (ATC,1996). On the other hand, the TESs may be classified as type B based on the ATC-40 system and hence, the R_A and R_V should be less than 2.27 and 1.79, respectively. In this study, both R_A and R_V are set to 1.5 (Yeh et al., 2000; Lin and Chang, 2003; Casarotti et al., 2009; Monteiro et al., 2014).

Third, the capacity curve taken from HAZUS is overlaid to compare with the inelastic response spectrum (see blue line in Figure 2). The capacity curves in HAZUS are defined based on two

engineering parameters, e.g. yield and ultimate strengths characterising the nonlinear (pushover) behavior of 36 building types (e.g. wood frame building to steel moment resisting frame). The building type classifications in HAZUS are based on the building material (e.g. wood, concrete and steel) and height. Therefore, following the HAZUS classification, the TESs in Padang are reinforced concrete moment resistant frames (RC-MRF) with different building heights. TESs no. 13 and 16 are considered to be high-rise RC-MRF (C1H), whereas the rest of TESs are mid-rise RC-MRF (C1M). Moreover, four seismic design code classifications including Pre-Code, Low-Code, Moderate-Code, and High-Code are defined corresponding to the seismic zone. In terms of seismic design code classification, High-Code is considered to be applicable to TESs in Padang, because Padang is located in the high seismic zone corresponding to the High-Code in HAZUS and TESs have been designed and constructed to higher standards/quality than other normal buildings. In the following, the seismic vulnerability assessment of TESs is carried out by focusing upon C1M because the C1H type is typically stronger than the C1M (i.e. for the same shaking intensity, C1H buildings are expected to perform better than CM1).

Finally, fragility curves developed in HAZUS are used to define the damage functions of the building. The probability of being in or exceeding a given damage state is modelled by a cumulative lognormal distribution. Four damage states, i.e. slight, moderate, extensive, and complete, are defined in HAZUS (see Figure 3). Subsequently, to determine whether a TES can be used for post-earthquake tsunami evacuation purposes (not for shelters), the building is categorised into safe and unsafe by referring to existing tagging criteria (FEMA-356, 2000; HAZUS, 2003; Bazzurro et al., 2006) including (see Figure 3):

- Green tag: the building may have experienced onset damage but is safe for immediate occupancy. The none-to-slight damage state is applicable.
- Yellow tag: re-occupancy of the building is restricted and limited access only is allowed. Moderate-to-extensive damage state corresponds to this case.

- Red tag: the building is unsafe and no access is granted, and will be in complete or collapse damage state.

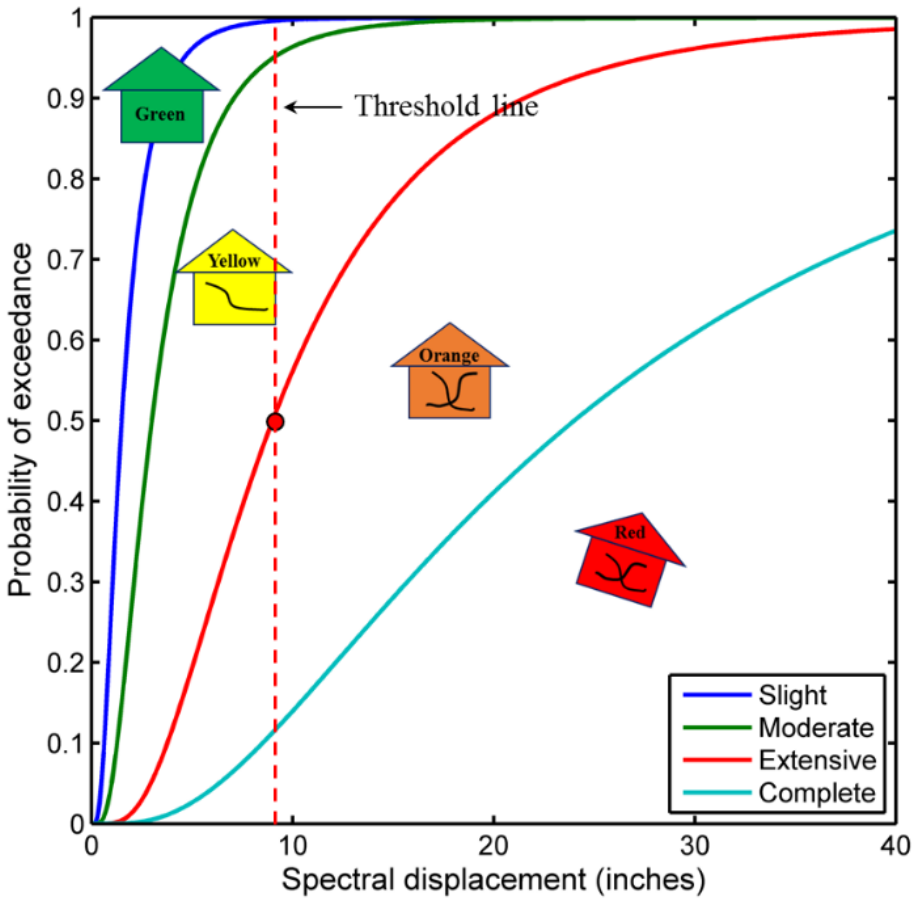

Figure 3. Fragility curves developed in HAZUS-MH (2001).

Based on the above tagging criteria, the tsunami evacuation building may be judged as unsafe for evacuation if the probability of extensive and complete damage states is over 50%. This assumption gives a 50-50 chance that the building may experience above or below extensive damage (Bazzurro et al., 2004, 2006). Moreover, the 50% probability of extensive or severer damage state is typically identified as the threshold value of a yellow tag in HAZUS that is adopted in this study (see Figure 3) and hence, may be regarded as the limit state to define the availability of evacuation buildings during the tsunami inundation.

For tsunami vulnerability assessment, Suppasri et al. (2011) models for RC structure is further used because of these reasons: 1) It was developed through extensive remote sensing and tsunami

survey data (i.e. ~5,000 points) in Banda Aceh and Thailand for the 2004 Indian Ocean tsunami; (2) the model is the most recent one among existing tsunami fragility models that are applicable to Sumatra, Indonesia; and (3) the model was successfully calibrated for the building vulnerability observed in the west coast of Thailand due to the 2004 Indian Ocean tsunami. These criteria are important because current situations of tsunami mitigation measures in Padang resemble those in Banda Aceh and Thailand more closely than situations in other regions. In Suppasri et al. (2011) model, only three damage states are adopted (see Figure 4) to generate fragility curves for reinforced concrete building including slight (DST1), moderate (DST2), and major/severe damage state (DST3). Using the calculated probability exceedance of each damage state, the TES is considered to be unsafe if the damage probability exceedance of major damage is above 50% (the major damage is assumed to be similar with the extensive damage in seismic damage state criteria).

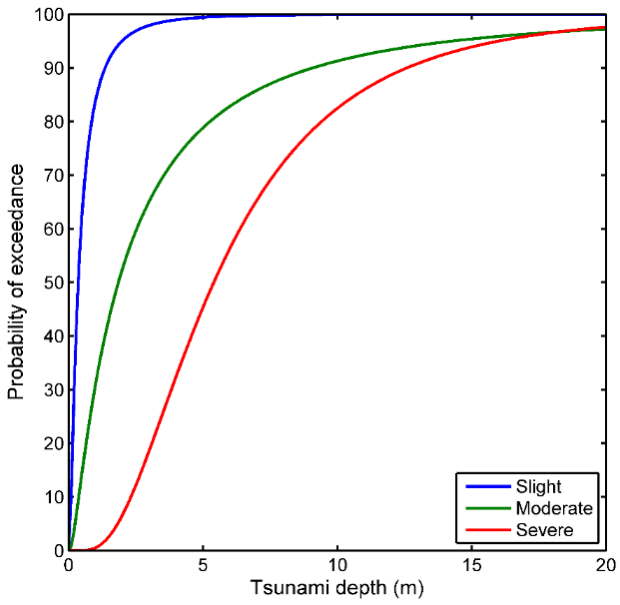

Figure 4. Tsunami fragility models developed by Suppasri et al. (2011)

3. RESULTS

For seismic vulnerability assessment, first, the earthquake-HAZUS vulnerability assessment using the median response spectra of the worst cases (i.e. using the closest distance of the possible 300 earthquake scenarios with the M_w 9.0) is presented in Figure 5. The median response spectra profile is

presented in Figure 5A. The ADRS is further calculated from the acceleration response spectrum as shown in Figure 5B. Using the ADRS, the capacity response spectrum method is implemented to determine the performance (demand) point (Figure 5C). The displacement performance point is estimated to be about 3 inches (7.6 cm) and then used to calculate the probability exceedance of damage states for a TES. Figure 5D shows that the sum of probabilities for extensive and complete damage states is ~7% and hence, the TES is considered to be safe for the median response spectra of the worst case.

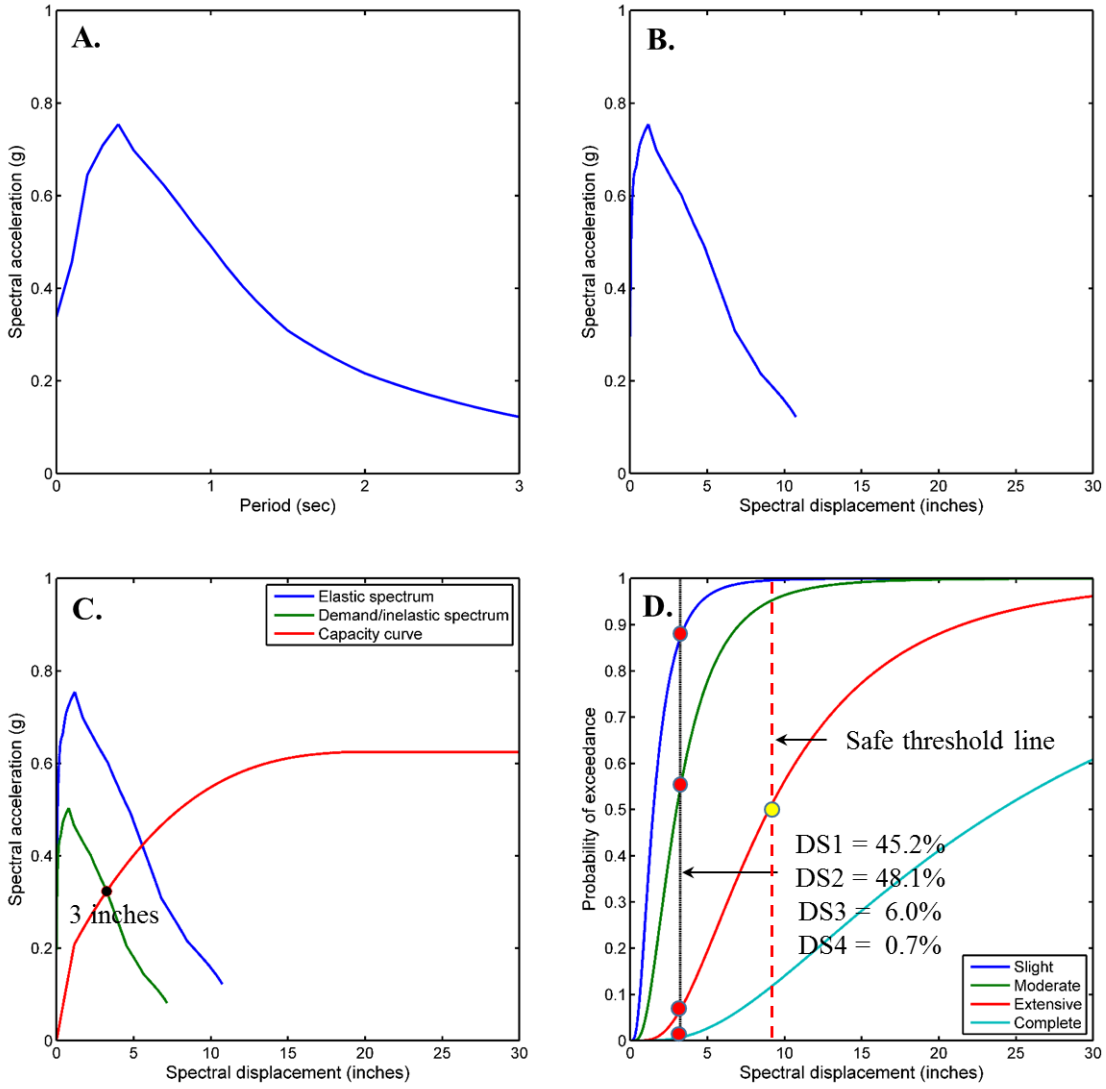

Figure 5. The seismic-HAZUS TES vulnerability assessment using the worst scenario.

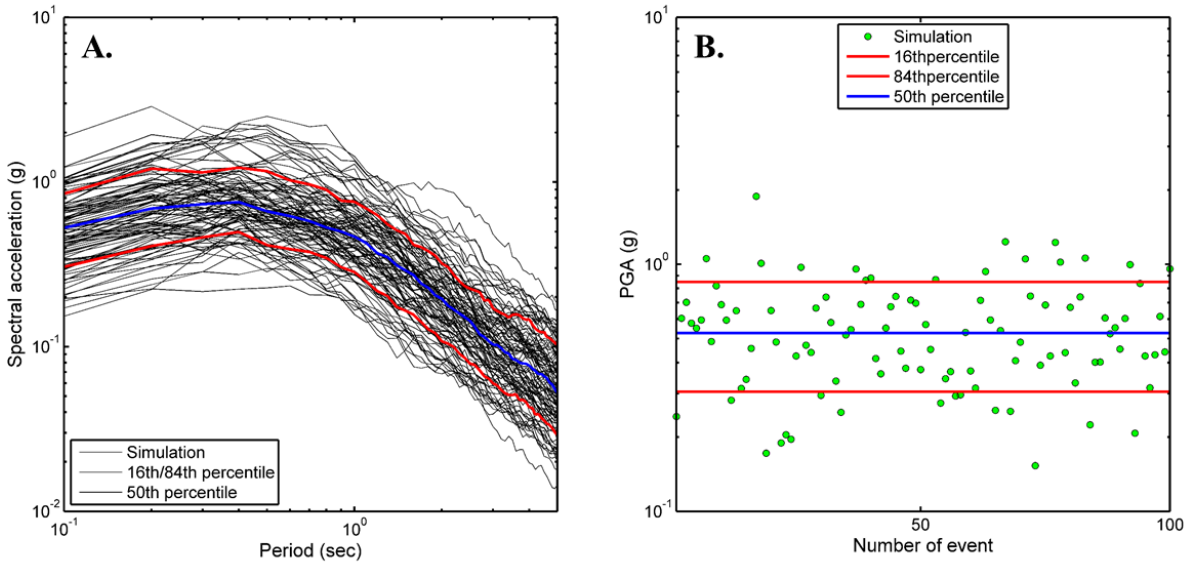

Figure 6. Earthquake simulation results from 100 tsunamigenic scenarios: (A). Spectral acceleration. (B). Peak Ground Acceleration (PGA).

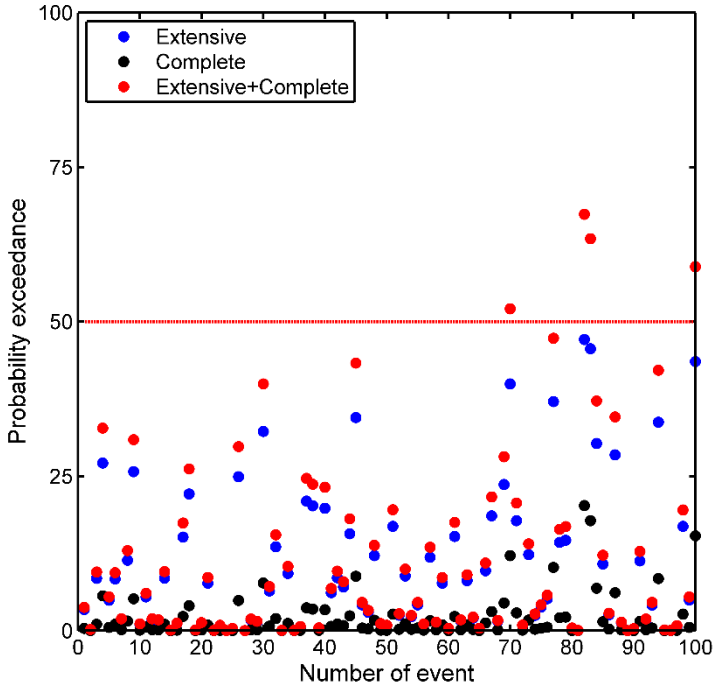

Figure 7. Probability exceedance of extensive and complete damage states for 100 seismic events.

Second, the results from a 100 tsunamigenic earthquake scenarios are presented in Figure 6. The spectral acceleration profile shows how large the ground shaking occurred in Padang, Indonesia

due to the 100 tsunamigenic earthquakes from the Mentawai segment of the Sunda subduction zone. The spectral acceleration profile (Figure 6A) from the 100 earthquake events shows that the range of Sa in Padang is in between 0.3 g to 0.9 g for the period below 1 s. Moreover, the PGA values (Figure 6B) is the interval of 0.3 g to 0.9 g with the median of about 0.5 g. Using the simulated response spectra from those 100 earthquake scenarios, the TES vulnerability is further performed. Figure 7 presents the probability exceedance of extensive (blue dot) and complete (black dot) damage states and the sum of these two probabilities (red dot). A 50% probability line is drawn to see the threshold of safe building. Figure 8 confirms that the TES may be operational for evacuation because ~95% from the total of 100 earthquake simulations produce less than 50% probability exceedance of above extensive damage state. Moreover, most of the cases results in less than 25% probability of exceedance above extensive damage state. Subsequently, the TES may be considered to be safe for evacuation after the ground shaking and hence, the tsunami vulnerability assessment can be carried out.

Fourth, the tsunami vulnerability assessment is performed. Using the maximum inundation depths at all 23 TESs from the 100 earthquake scenarios of the M_w 9.0, the probability of exceeding severe damage state (DST3) of each TES is calculated. In this study, the number of event producing the probability of exceeding severe damage state of more than 50% is defined as destructive event. The destructive events for the shelter numbers 16 and 17 are relatively large, i.e. 30% and 36% of the 100 events are destructive for the shelter numbers 16 and 17, respectively and hence, these two shelters may be considered to be unsafe for the evacuation. Moreover, the percentage of non-destructive event for the other shelters are above 75%. Therefore, except for shelter number 16 and 17, the rest of the shelters consider to be operational for evacuation.

References

Abrahamson, N., Gregor, N., and Addo, K.: BC hydro ground motion prediction equations for subduction earthquakes. Earthquake Spectra 32, 23–44. doi: 10.1193/051712EQS188MR, 2016.

Applied Technology Council, : Seismic Evaluation and Retrofit of Concrete Buildings, Report ATC 40, November, 1996.

Ahmad, S., Kyriakides, N., Pilakoutas, K., Neocleous, K., and Zaman, Q. : Seismic fragility assessment of existing sub-standard low strength reinforced concrete structures, Earthq. Eng. Eng. Vib., 14, 439. https://doi.org/10.1007/s11803-015-0035-0, 2015.

Baker, J. W. and Cornell, C. A.: Correlation of response spectral values for multicomponent ground motions, Bull. Seismol. Soc. Am., 96, 215-227.

Bazzurro, P, Cornell, C. A., Menun, C, and Motahari, M.: Guidelines for seismic assessment of damaged buildings, the 13th World Conference on Earthquake Engineering, Vancouver, Canada, 1-6 August, 2004.

Bazzurro, P, Cornell, C. A., Menun, C, and Motahari, M.: Advanced seismic assessment guidelines, Pacific Earthquake Engineering Research Centre, Stanford University, 2006.

Briggs, R.W., Sieh, K., Meltzner, A.J., Natawidjaja, D., Galetzka, J., Suwargadi, B., Hsu, Y., Simons, M., Hananto, N., Suprihanto, I., Prayudi, D., Avouac, J.P., Prawirodirdjo, L., and Bock, Y. (2006). Deformation and slip along the Sunda megathrust in the great 2005 Nias-Simeulue earthquake. Science 311, 1897–1901. doi:10.1126/science.1122602.

Borrero, J. C., Sieh, K., Chlieh, M., and Synolakis, C. E.: Tsunami inundation modeling for western Sumatra, Proc. Nat. Acad. Sci. U.S.A., 103, 19673–19677, doi:10.1073/pnas.0604069103, 2006.

De Risi, R. and Goda, K.: Probabilistic Earthquake–Tsunami Multi-Hazard Analysis: Application to the Tohoku Region, Japan. Front. Built Environ., 2, 25, doi: 10.3389/fbuil.2016.00025, 2016.

Douglas, J and Gkimprixis, A.: Using targeted risk in seismic design codes: a summary of the state of the art and outstanding issues, 6th National Conference on Earthquake Engineering and 2nd National Conference on Earthquake Engineering and Seismology, Bucharest, Romania, 14/06/17 - 17/06/17, 3-10, 2017.

FEMA (Federal Emergency Management Agency) 356: Pre-standard and commentary for the seismic rehabilitation of buildings, Federal Emergency Management Agency, Washington, D.C., 2009.

HAZUS. Multi-hazard Loss Estimation Methodology Earthquake Model. Federal Emergency Management Agency, Washington, D.C., 2003.

Iwasaki, T. and Mano, A.: Two-dimensional numerical computation of tsunami run ups in Eulerian description, Proc. Of 26th Conference on Coastal Engineering, Japan, JSCE, 70-74.

Meltzner, A.J., Sieh, K., Abrams, M., Agnew, D. C., Hudnut, K.W., Avouac, J.P., and Natawidjaja, D. H. (2006). Uplift and subsidence associated with the great Aceh-Andaman earthquake of 2004. J. Geophys. Res. 111, B02407, doi:10.1029/2005JB003891.

Monecke, K., Finger, W., Klarer, D., Kongko, W., McAdoo, B. G., Moore, A. L., and Sudrajat, S.U. (2008). A 1,000-year sediment record of tsunami recurrence in northern Sumatra. Nature 455, 1232–1234. doi:10.1038/nature07374.

Mori N, Muhammad A, Goda K, Yasuda T and Ruiz-Angulo A (2017) Probabilistic Tsunami Hazard Analysis of the Pacific Coast of Mexico: Case Study Based on the 1995 Colima Earthquake Tsunami. Front. Built Environ. 3:34. doi: 10.3389/fbuil.2017.00034.

Muhari, A., Imamura, F., Koshimura, S., and Post, J.: Examination of three practical run-up models for assessing tsunami impact on highly populated areas, Nat. Hazards Earth Syst. Sci., 11, 3107-3123, doi:10.5194/nhess-11-3107-2011, 2011.

Muhari, A., Imamura, F., Natawidjaja, D. H., Diposaptono, S., Latief, H., Post, J., and Ismail, F.A.: Tsunami mitigation efforts with pTA in West Sumatra Province, Indonesia. J. Earthq. Tsunami, 4, 341–368, doi:10.1142/S1793431110000790, 2010.

Natawidjaja, D.H., Sieh, K., Chlieh, M., Galetzka, J., Suwargadi, B.W., Cheng, H., Edwards, R.L., Avouac, J.P., and Ward, S.N. (2006). Source parameters of the great Sumatran megathrust earthquakes of 1797 and 1833 inferred from coral microatolls. J. Geophys. Res. 111, B06403, doi:10.1029/2005JB004025.

Rossetto, T. and Elnashai, A.: Derivation of vulnerability functions for European-type RC structures based on observational data, Eng. Str., 25, 1241-1263, 2003.

Sarabandi, P., Pachakis, D., King, S., and Kiremidjian, A.: Empirical fragility functions from recent earthquakes. The 13th world conference in Earthquake Engineering, Vancouver, Canada, August 1-6, 2004.

Sengara, I. W, Sidi, I. D, Mulia, A, Muhammad, A, and Daniel H.: Development of risk coefficient for input to new Indonesian seismic building codes. Journal of Engineering and Technological Sciences, 48, 49–65, 2016.

Sieh, K., Natawidjaja, D.H., Meltzner, A.J., Shen, C.C., Cheng, H., Li, K.S., Suwargadi, B.W., Galetzka, J., Philibosian, B., and Edwards, R.L. (2008). Earthquake super cycles inferred from sea-level changes recorded in the corals of West Sumatra. Science 322, 1674–1678. doi:10.1126/science.1163589.

Wijayanti, E, Kristiawan, S. A, Purwanto, E, and Sangadji, S.: Seismic Vulnerability of Reinforced Concrete Building Based on the Development of Fragility Curve: A Case study, Applied Mechanics and Materials, 845, 252-258, 2015.

Zachariasen, J., Sieh, K., Taylor, F.W., Edwards, R.L., and Hantoro, W.S. (1999). Submergence and uplift associated with the giant 1833 Sumatran subduction earthquake: Evidence from coral microatolls. J. Geophys. Res. 104, 895–919.